Supplementary Tables

Table S1. Position of the mariner transposon insertion in *xerC* and *nth* genes.

Clone	Gene	Nucleotide position in the N16961 genome	Flanking DNA sequence
1	*xerC*	122149	tacttTA-------
2	*xerC*	122486	gagcTA-------
3	*xerC* (promotor)	121393	atcttTA-------
4	*xerC*	122120	aattaTA-------
5	*xerC*(promotor)	121988	gacatTA
6	*xerC*	122149	gtactTA
7	*nth*	1080611	ccgcaTA-------
8	*nth*	1080773	acggcCA-------
9	*nth*	1080523	gttttTA-------
10	*nth*	1080511	tgctcTA-------
11	*nth*	1080611	ttgagTA-------

Table S2. Strains

Strains	Genotype/Phenotypes	References/ Resources
N16961	O1 El Tor strain, St^r	(Heidelberg et al., Nature, 2000)
MV18	N16961 *lacZ* (RS2 RS1 *dif*1)::*aadA1*; Sp^r St^r	(Das et al., PNAS, 2010)
MV78	MV18 $lacZ_{Ec}$::*dif1*; St^r	(Das et al., PNAS, 2010)
BJ51	MV78 *fpg::arr2* ; Ery^r	This study
BJ52	MV78 *nth::*Km^r	This study
BJ53	MV78 *fpg::arr2, nth::*Km^r ; Ery^r	This study
BJ47	MV78 *xthA*::Km^r	This study
BJ48	MV78 *nfo*	This study
BJ78	MV78 *nfo, xthA*::Km^r	This study

Table S3. Oligonucleotides used in this study. Nucleotides highlighted in bold correspond to the overlap region of the different recombination sites.

Name	Sequence
Diftop	ATCAGTGCGCATTATGTATGTTATGTTAAATGGA
Difbot	CTGTCCATTTAACATAACATACATAATGCGCACTGAT
AttPtop	TACGCCCTTAGTGCGTATTATGTGGCGCGGCATTATGTTGAGGGTTCCG
AttPbot	CTGCGGAACCCGTAACATAATGGCGTATAATACGCATTAAGGGCGTA
DiftopEXT	CAATCTAGACCGCCGCCTTAGTGCGCATTATGTATGTTATGTTAAATTAAGGCATAATGTCGACAA
DifbotEXT	TTGTCGACATTATGCCTTAATTTAACATAACATACATAATGCGCACTAAGGCGGCGGTCTAGATTG
HJ-CTX1	GATCCGTGATCACGCTGAACGCGTTTTAGCAGTGCGCATTATGTGGCGCGGCATTATGTTGAGGGGCCTAACGCCTAAAGCGGCCGCCTA
HJ-CTX2	ATCGTAGGCGGCCGCTTTAGGCGTTAGGCCCCGTAACATAATGGCGTATAATACGCATTCGACCGTTGCCGGATCCG
HJ-CTX3	CGATCGGATCCGGCAACGGTCGAGTGCGTATTATGTATGTTATGTTAAATGACATCCTGAGATCTCGA
HJ-X4	TCGATCGAGATCTCAGGATGTCATTTAACATAACATACATAATGCGCACTGCTAAAACGCGTTCAGCGTGATCACG
HJ-CTX2	ATCGTAGGCGGCCGCTTTAGGCGTTAGGCCCCGTAACATAATGGC

suicide	GTCTAATACGCATTCGACCGTTGCCGGATCCG
HJ-X4 suicide	TCGATCGAGATCTCAGGATGTCATTTAACATAACATATCTAATGCG CACTGCTAAAACGCGTTCAGCGTGATCACG
HJ-DIF-1	GATCCGTGATCACGCTGAACGCGTTTTAGCAGTGCGCATTATGTAT GTTATGTTAAATGGCCTAACGCCTAAAGCGGCCGCCTA
HJ-DIF-2	ATCGTAGGCGGCCGCTTTAGGCGTTAGGCCATTTAACATAACATAC ATAATGCGCACTCGACCGTTGCCGGATCCG
HJ-DIF-3	CGATCGGATCCGGCAACGGTCGAGTGCGCATTATGTATGTTATGTT AAATGACATCCTGAGATCTCGA
K120QTop	GCCCGGCGTTGGGCGTCAAACCGCTAATGTGGTG
K120QBot	CACCACATTAGCGGTTTGACGCCCAACGCCGGGC
NSpe Top	GCCCGGCGTTGGGCGTAGCACCGCTAATGTGGTGTTG
NSpe Bot	CAACACCACATTAGCGGTGCTACGCCCAACGCCGGGC
FORK-1	CGCGGTACGGCCGGAAGCCTGCTTTTTTATACAAGCTTAACTCCC
FORK-2	GCGTCGGCTGCAGAGCGTATAAAGCAGGCTTCCGGCCGTACCGCG
FORK-3	GGGAGTTAAGCTTGTATAAA
FORK-4	ATACGCTCTGCAGCCGACGC
ARB1	GGCCACGCGTCGACTAGTACNNNNNNNNNNGATAT
ARB2	GGCCACGCGTCGACTAGTAC
ARB6	GGCCACGCGTCGACTAGTACNNNNNNNNNNACGCC
1314	GTCATCGTCATCCTTGTAATCG
846	AAATGATCACGAGATAGGGTTGAGTGTTG

Table S4. Plasmids

Name	Description	References/Resources
pSW23T	pSW23::oriTRP4; oriVR6Kγ; Cm^r	(Demarre et al., Res Microbiol, 2005)
pKAS32	pGP704 derivative carrying the *rps*L counter selectable marker; Ap^r	(Skorupski and Taylor, Gene, 1996)
pMEV30	pSW23T harbouring the replication and integration machinery of RS1, a CTX satellite phage of *V. cholerae strain* N16961; Cm^r	(Das et al., PNAS, 2010)
pSW-Short- CTX	$AttP^{ET}$ cloned into pSW23T	(Val et al., Mol Cell, 2005)
pBJ13	pSC101 derivative with nth^{Vc} under P_{ara} promoter	This study
pBJ14	pSC101 derivative with nth^{Ec} under P_{ara} promoter	This study
pBJ16	pKAS32 carrying an Km^R cassette flanked by the upstream and downstream regions of *nth*; Ap^r	This study
pBJ18	pKAS32 carrying an Km^R cassette flanked by the upstream and downstream regions of *xthA*; Ap^r	This study
pBJ20	pKAS32 carrying an Ery^R cassette flanked by the upstream and downstream regions of *fpg*; Ap^r	This study
pBJ41	pSC101 derivative with nei^{Ec} under P_{ara} promoter	This study

pBJ42	pSC101 derivative with *nth*^{Vc} *(K120Q)* under P_{ara} promoter	This study
pBJ61	pET28a vector with EndoIII Vcholerae gene cloned NcoI/XhoI	This study
pBJ62	pBJ61 with the K120Q mutation into EndoIII	This study
pBS22	pSW23T harbouring the replication and integration machinery RS2 of the CTX classical phage of *V. cholerae* strains 569B; Cm^r	(Das et al., PNAS, 2010)

References

Das, B., Bischerour, J., Val, M.-E., and Barre, F.X. (2010). Molecular keys of the tropism of integration of the cholera toxin phage. PNAS *107*, 4377-4382.

Demarre, G., Guerout, A.M., Matsumoto-Mashimo, C., Rowe-Magnus, D.A., Marliere, P., and Mazel, D. (2005). A new family of mobilizable suicide plasmids based on broad host range R388 plasmid (IncW) and RP4 plasmid (IncPalpha) conjugative machineries and their cognate Escherichia coli host strains. Res Microbiol *156*, 245-255.

Heidelberg, J.F., Eisen, J.A., Nelson, W.C., Clayton, R.A., Gwinn, M.L., Dodson, R.J., Haft, D.H., Hickey, E.K., Peterson, J.D., Umayam, L., *et al*. (2000). DNA sequence of both chromosomes of the cholera pathogen Vibrio cholerae. Nature *406*, 477-483.

Kepple KV, Boldt JL, Segall AM (2005) Holliday junction-binding peptides inhibit distinct junction-processing enzymes. *Proc Natl Acad Sci U S A* **102**(19)**:** 6867-6872

Skorupski, K., and Taylor, R.K. (1996). Positive selection vectors for allelic exchange. Gene *169*, 47-52.

Thayer MM, Ahern H, Xing D, Cunningham RP, Tainer JA (1995) Novel DNA binding motifs in the DNA repair enzyme endonuclease III crystal structure. *EMBO J* **14**(16)**:** 4108-4120

Val, M.-E., Bouvier, M., Campos, J., Sherratt, D.J., Cornet, F., Mazel, D., and Barre, F.-X. (2005). The single stranded genome of phage CTX is the form used for integration into the genome of *Vibrio cholerae*. Mol Cell *19*, 559-566.

Supplementary Figures

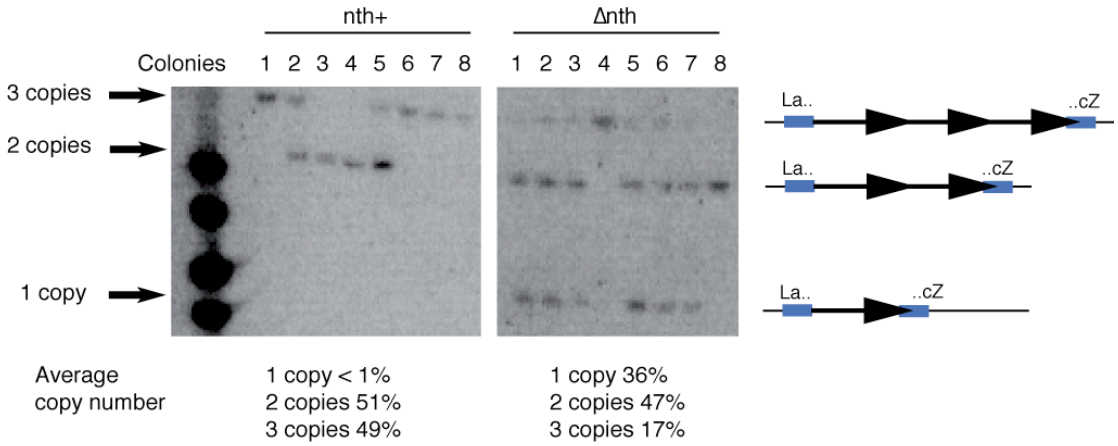

Figure S1. Detection of the number of integrated copies of RS1 found in N16961 reporter cells after lysogenic conversion. Briefly, 8 individual white colonies (lysogenic clones) from a WT or a *nth* genetic background were grown overnight. Genomic DNA was extracted and 5µg of DNA was digested by AvaI (10 units, New England Biolabs) for 5 hours. Restriction products were separated on a 0.8% agarose, 1X TAE gel. Southern Blot was performed using a radioactively labeled probe against the *lacZ* gene. The pMEV30 (containing RS1) is devoid of AvaI restriction sites. Genomic DNA digested by AvaI generates a 1580bp fragment encompassing the *LacZ*::*dif* cassette in the absence of lysogenic phage or DNA fragments of 6381bp, 11182bp and 15983bp when 1 copy, 2 copies and 3 copies of the phage are integrated, respectively. The signals corresponding to a single integrated copy in the 8 colonies that were analysed were added. The signals corresponding to double integrated copies in the 8 colonies that were analysed were added. The signals corresponding to triple integrated copies in the 8 colonies that were analysed were added. The fraction of the genomes containing 1, 2 and 3 copies were obtained by dividing these numbers by the total signal detected. Fractions are indicated at the bottom of the gels.

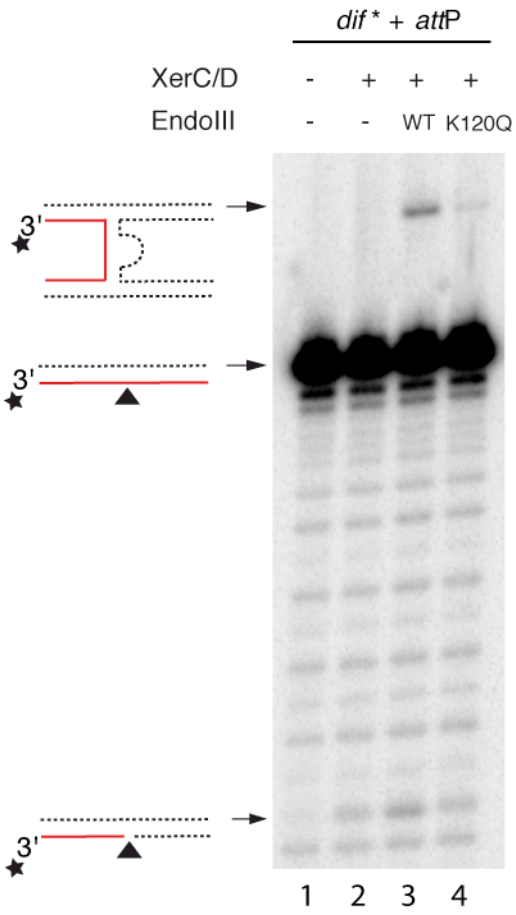

Figure S2. *Vibrio cholerae* EndoIII and the K120Q mutant stimulate recombination between *dif and att*P of RS2. 3' labelled *dif* and cold *att*P substrates were incubated with XerC and XerD recombinases with the wild type or the K120Q mutant *V.cholerae* EndoIII. Reactions were incubated for 4 hours at 37°C. Samples were ethanol precipitated and the different products were separated on a 10% acrylamide sequencing gel. Schemes of the *att*P/*dif* pseudo-HJ product generated by XerC catalysis and the cleaved intermediate are shown on the left of the gel. The 3' labeled strands is colored in red. *Vibrio cholerae* EndoIII sequence is 85% identical to the *E. coli* protein. The *Vibrio cholerae* protein stimulates efficiently the reaction (compare lane 2 and 3). The K120Q mutant is catalytically dead (k_{cat} 10000 fold reduce (Thayer et al, 1995)) but it continues to stimulate the reaction (compare lane 2 and 4) demonstrating that the catalytic activity of EndoIII is not essential. Nevertheless, the K120Q mutation reduces the ability to stimulate the recombination suggesting that this residue is somehow critical for this novel activity of EndoIII.

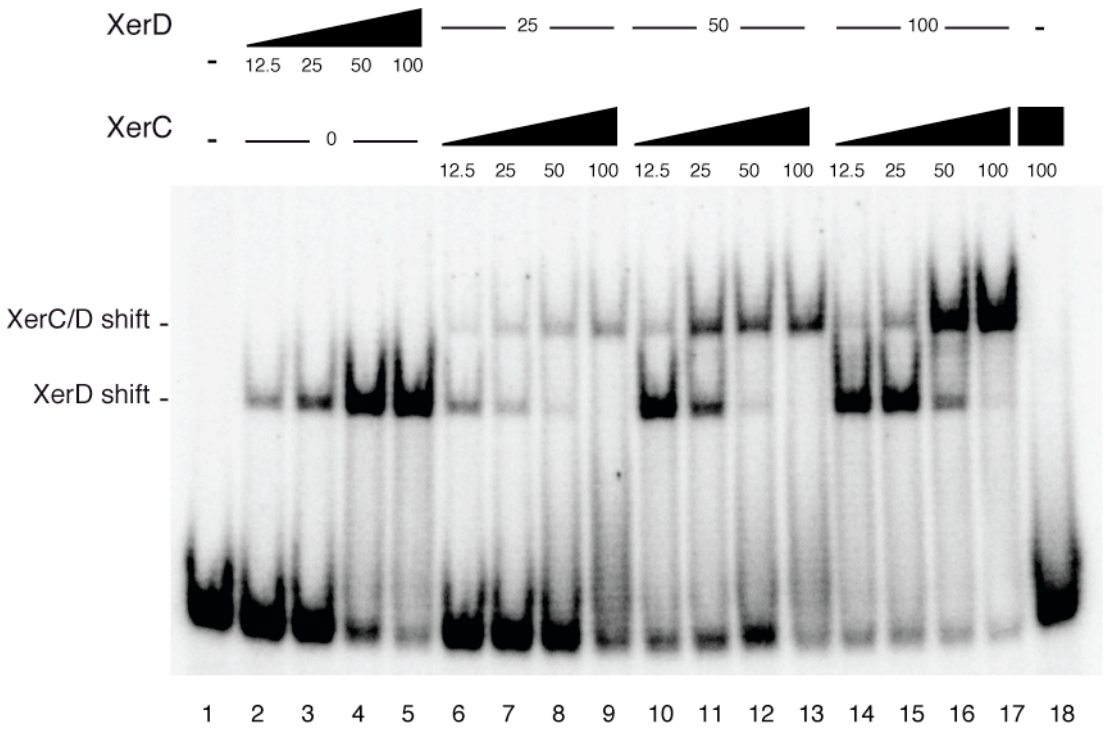

Figure S3. XerD stimulates XerC binding on *dif*1 DNA sequences.
XerC and XerD DNA binding activity on *dif*1 double strand DNA substrate was evaluated by electrophoretic mobility shift assay (EMSA). Assay was performed with 10nM *dif*1 DNA labelled substrate in the reaction buffer containing 25mM Tris-HCl (pH 7.4), 100mM NaCl, 1mM EDTA, 0.1µg/mL BSA and 10% glycerol. Samples were incubated 5 minutes at room temperatures before loading on a 5% acrylamide, 1X TBE gel and run at RT during 45 minutes. Gel was dried, exposed to phosphorscreen and analysed using Typhoon (GE Healthcare). DNA substrate was first titrated using increasing concentration of XerD alone (lanes 1 to 6). In similar conditions, XerC (100nM) alone does not bind to *dif*1 (see lane 18). EMSA was then repeated in the presence of XerD (25, 50 or 100nM) and increasing concentrations of XerC (12,5, 25, 50, 100nM). XerC/D-*dif*1 complexes are formed efficiently even at 12,5nM concentrations of XerC (see lanes 6, 10, 14) further demonstrating that XerC is highly dependant of XerD for *dif*1 DNA binding.

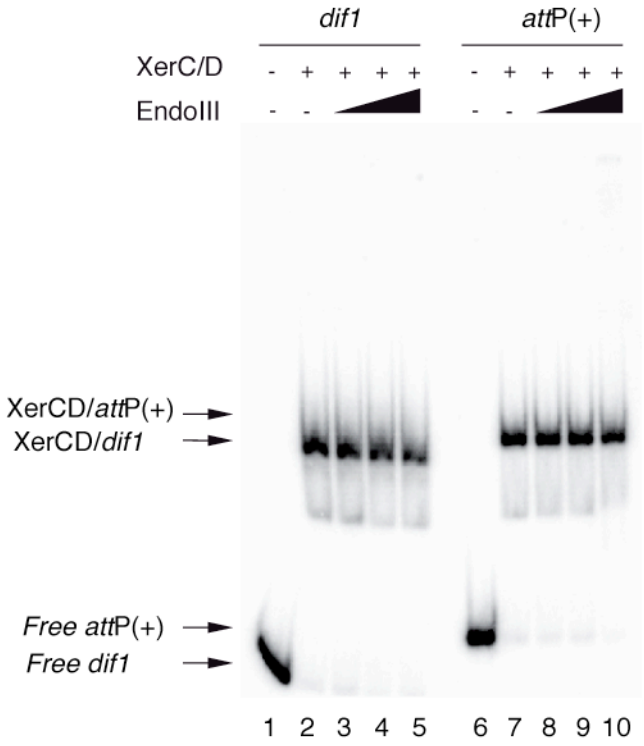

Figure S4. (**A**) EMSA of *dif*1 in the presence of XerC, XerD and/or Endo III. (**B**) EMSA of *att*P(+)in the presence of XerC, XerD and/or Endo III. Experiments were performed as in Figure 5A.

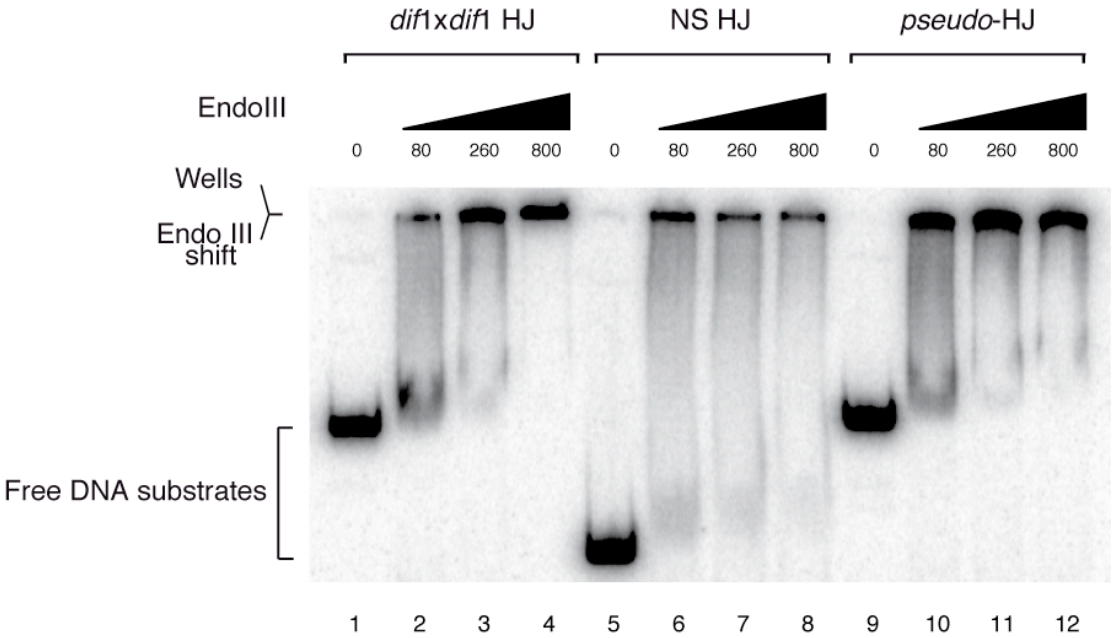

Figure S5. Endo III binds to HJs independently of their sequence.
EMSA of *dif*1/*dif*1 HJs, non specific HJs (NS-HJ) and *att*P(+)/*dif*1 pseudo–HJs in the presence of increasing concentrations of Endo III (0 lanes 1, 5 and 9, 80nM lanes 2, 6 and 10, 260nM lanes 3, 7 and 11 and 800nM lanes 4, 8 and12). The sequences of the NS HJ are identical to those described by (Kepple et al, 2005). Samples were incubated 5 minutes at room temperatures before loading on a 5% acrylamide, 1X TBE gel and run at 4°C during 45 minutes. Gel was dried, exposed to phosphorscreen and analysed using Typhoon (GE Healthcare).

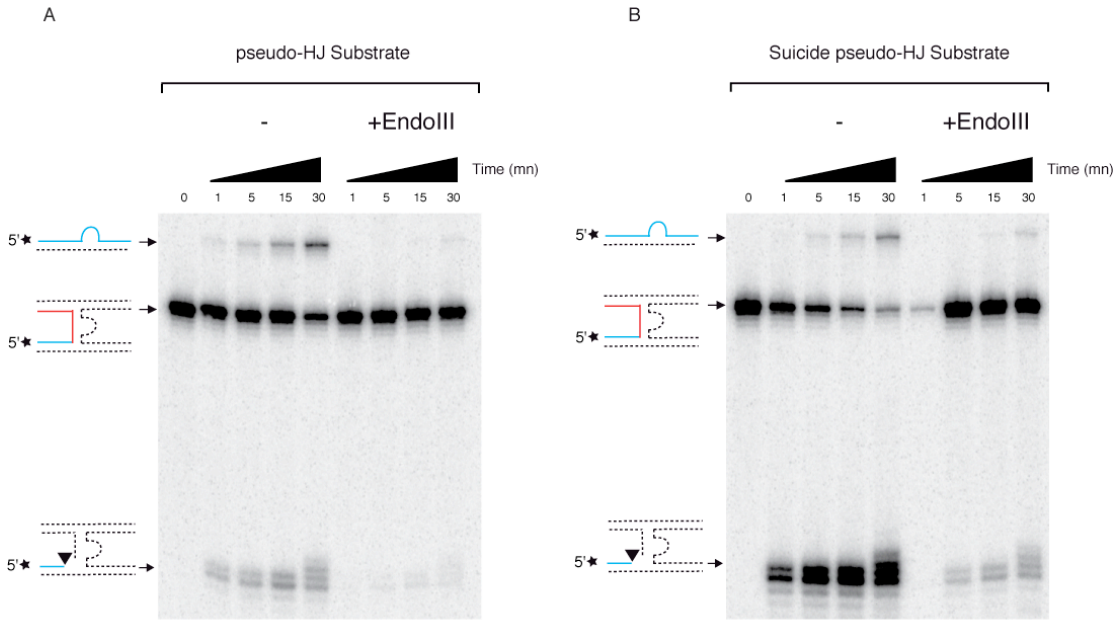

Figure S6. EndoIII blocks XerC cleavage step of the pseudo-HJ resolution. (A) Pseudo-HJ resolution assays were performed in the presence or the absence of EndoIII. Pseudo-HJ DNA substrates were radiolabelled at the 5' extremity of the HJ-III strand. Assay was performed with 10nM of the *att*P(+)/*dif*1 pseudo–HJs, 100nM XerD and 150nM XerC in the reaction buffer containing 25mM Tris-HCl (pH 7.4), 100mM NaCl, 1mM EDTA, 0.1µg/mL BSA and 10% glycerol. When present, EndoIII was added at 200nM concentration immediately after XerC and XerD recombinases. Aliquots of the reaction were removed 1, 5, 15 and 30 minutes after the addition of the recombinases. The reaction was stopped by the addition of 0,1% SDS and proteinase K. Samples were treated and resolved on 10% acrylamide denaturing gel. Gel was dried, exposed to phosphorscreen and analysed using Typhoon (GE Healthcare). Schemes of the XerC cleaved intermediate and the resolved *att*P(+) substrates are depicted on the left. In the presence of EndoIII, the cleaved intermediate failed to accumulate, suggesting that EndoIII inhibit the reaction at a early step of the reaction. **(B)** Pseudo-HJ resolution assays were performed using a suicide pseudo-HJ. The conditions of the assay are similar to those of the figure A, except that the pseudo-HJ *att*P(+)/*dif*1 was replaced by the suicide substrate depicted in figure 6A.

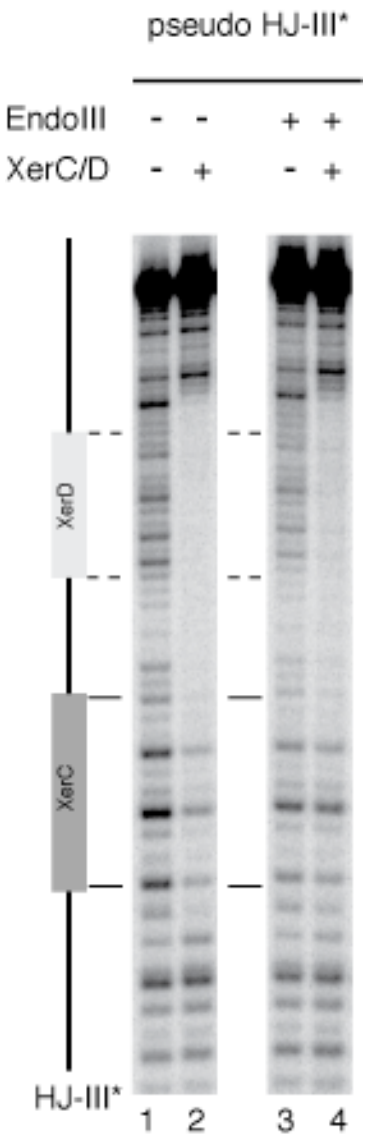

Figure S7. EndoIII displaces XerC from the pseudo-HJ.
DNaseI footprint experiment was performed using the pseudo-HJ labelled at the 5' extremity of the HJ-III strand (cleaved by XerC). Experiment was performed in conditions similar to those of the figure 6C (see Material and methods), in the presence of XerC/D (lane 2 and 4) and/or EndoIII (lanes 3 and 4). XerC and in a more limited way XerD footprint is lost after addition of EndoIII (compare lanes 2 to 1 and 4 to 3), supporting the hypothesis that the binding of EndoIII to the pseudo-HJ displaces XerC from it.

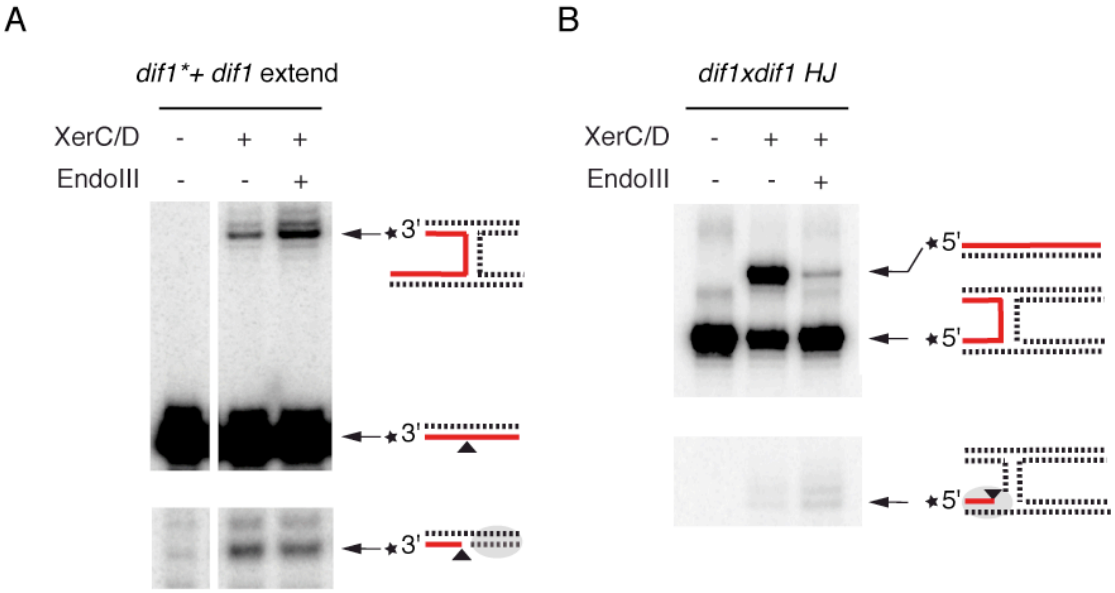

Figure S8. (A) EndoIII stimulates the formation of the *dif*/*dif* HJ. The conditions of the assay were similar to those of the Figure 4D. A labeled substrate was reacted with the *dif* extended substrate. (**B**) EndoIII inhibits the resolution of a the *dif*/*dif* HJ by XerC-mediated strand exchanges. The conditions of the assay were similar to those of Figure 4E except that the *attP*/*dif* pseudo-HJ was replaced by a *dif*/*dif* HJ.

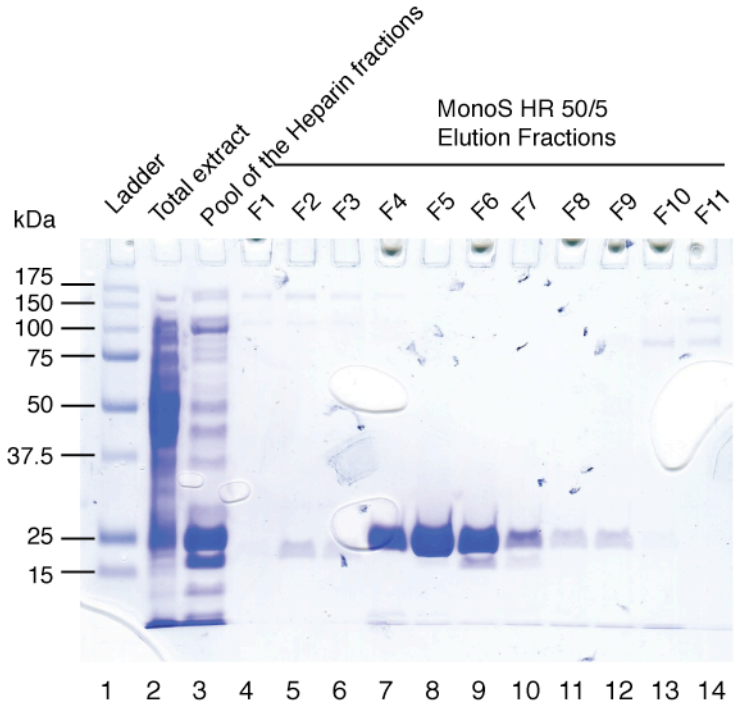

Figure S9. SDS-PAGE analysis of the protein samples during the course of *V.cholerae* EndoIII purification. Lane 1: Protein Ladder, 2: Protein extract of *V.cholerae* EndoIII producing cells 3: EndoIII containing fractions after heparin column purification, 4-14: Elution fractions of the MonoS column. EndoIII elutes in the fraction F5 and was estimated to be over 95% pure according to coomassie blue staining. Samples were analysed on 12% acrylamide Tris-Glycine gel.